

Fluid Antenna System: New Insights on Outage Probability and Diversity Gain

Wee Kiat New, *Member, IEEE*, Kai-Kit Wong, *Fellow, IEEE*,
 Hao Xu, *Member, IEEE*, Kin-Fai Tong, *Fellow, IEEE*,
and Chan-Byoung Chae, Fellow, IEEE

Abstract

To enable innovative applications and services, both industry and academia are exploring new technologies for sixth generation (6G) communications. One of the promising candidates is fluid antenna system (FAS). Unlike existing systems, FAS is a novel communication technology where its antenna can freely change its position and shape within a given space. Compared to the traditional systems, this unique capability has the potential of providing higher diversity and interference-free communications. Nevertheless, the performance limits of FAS remain unclear as its system properties are difficult to analyze. To address this, we approximate the outage probability and diversity gain of FAS in closed-form expressions. We then propose a suboptimal FAS with N^* ports, where a significant gain can be obtained over FAS with $N^* - 1$ ports whilst FAS with $N^* + 1$ ports only yields marginal improvement over the proposed suboptimal FAS. In this paper, we also provide analytical and simulation results to unfold the key factors that affect the performance of FAS. Limited to systems with one active radio frequency (RF)-chain, we show that the proposed suboptimal FAS outperforms single-antenna (SISO) system and selection combining (SC) system in terms of outage probability. Interestingly, when the given space is $\frac{\lambda}{2}$, the outage probability of the proposed suboptimal FAS with one active RF-chain achieves near to that of the maximal ratio combining (MRC) system with multiple active RF-chains.

The work of W. K. New, K.-K. Wong and K.-F. Tong is supported by the Engineering and Physical Sciences Research Council (EPSRC) under grant EP/W026813/1. The work of C.-B. Chae is supported by the Institute for Information and Communication Technology Promotion (IITP) grant funded by the Ministry of Science and ICT (MSIT), Korea (No. 2021-0-02208, No. 2021-0-00486). The work of H. Xu is supported by the European Union's Horizon 2020 Research and Innovation Programme under Marie Skłodowska-Curie Grant No. 101024636.

Wee Kiat New (email: a.new@ucl.ac.uk), Kai-Kit Wong (email: kai-kit.wong@ucl.ac.uk), Hao Xu (email:hao.xu@ucl.uk), and Kin-Fai Tong (email: k.tong@ucl.ac.uk) are with the Department of Electronic and Electrical Engineering, University College London, London WC1E 6BT, United Kingdom.

Chan-Byoung Chae (email: cbchae@yonsei.ac.kr) is with the School of Integrated Technology, Yonsei University, Seoul 03722 Korea. Kai-Kit Wong is also affiliated with Yonsei Frontier Lab., Yonsei University, Seoul 03722, Korea.

Index Terms

6G, fluid antenna system, outage probability, diversity gain, performance analysis.

I. INTRODUCTION

Fifth generation (5G) wireless networks have recently been deployed worldwide and thus the industry and academia are now looking for new technologies to maximize the potentials of sixth generation (6G) wireless networks. One of the promising candidates is fluid antenna system (FAS). Unlike traditional antenna systems, FAS is a software-controllable fluidic, conductive or dielectric structure that can freely adjust its position and shape within a given space [1]. The most basic single fluid antenna consists of one radio frequency (RF)-chain and N preset positions (known as ports) that are distributed within a given space while more advanced designs are also possible. The fluid radiator can freely switch its position among these ports to obtain a stronger channel gain, lower interference, and other desirable performance [2].

Fluid antenna is now feasible thanks to the recent advancement of using liquid metals and ionized solutions for antennas. Some prototypes can be found in [3]–[6]. As discussed in [7], other flexible antenna structures such as software-controlled pixel antenna or movable antenna can also be considered as fluid antenna. In essence, the key principle of FAS is to exploit its dynamic position and shape to achieve ultimate diversity and multiplexing gains [7]. Moreover, in the future, FAS can be applied together with other 6G candidates such as re-configurable intelligent surfaces (RIS), massive multiple-input multiple-output (MIMO) and terahertz (THz) communications. In particular, FAS can help to reduce the optimization complexity of RIS [1], improve the multiplexing gain of massive MIMO [8] and combat the high path loss effect of THz communications [9].

Despite its advantages, the fundamental limits of FAS and key factors that affect its performance remain unclear. One of the reasons is because the channels of FAS are strongly correlated since the ports can be closely placed to each other. Consequently, the probability density function (PDF) and cumulative distribution function (CDF) of FAS channels are intractable [10]. As a result, the outage probability and diversity gain of FAS are not known in closed-form expressions. In addition, increasing the number of ports of FAS has an inherit diminishing gain due to

one active RF-chain [11].¹ Thus, a suboptimal number of ports that are required to achieve a satisfactory performance is not known. Yet, this number is practically and theoretically important as it reduces the implementation challenges and analysis complexity.

Conceptually, FAS can be viewed similar to a traditional selection combining (SC) system since both systems use only one active RF-chain and there is a set of ports (i.e., FAS) or antennas (i.e., SC) to select from. Nevertheless, unlike traditional SC system, FAS can have infinitely many ports in a limited space (e.g., when using liquid metals) which makes the implementation and analysis much more challenging. In addition, the unique capability of freely switching the radiating element among the ports can be exploited to mitigate multi-user interference. These features are impractical in traditional SC systems.

State-of-the-arts show that FAS outperforms maximal ratio combining (MRC) system if the number of ports is sufficiently large [7]. In fact, [7] proves that FAS achieves arbitrarily small outage for a fixed rate/signal-to-noise ratio (SNR) as $N \rightarrow \infty$. In [12], the authors reveal that the ergodic capacity of FAS increases with N and thus FAS can outperform MRC in terms of ergodic capacity. Interestingly, FAS can also be used for multiple access. Specifically, [13] proposes a fluid antenna multiple access (FAMA) system which leverages the moment of deep fades in space to reduce multi-user interference. Motivated by these works, [14] employs stochastic geometry to analyze the outage probability of FAS in large-scale downlink cellular networks and [15] analyzes the performance of FAS in a more general correlated fading channel.

Nevertheless, [16] alludes that the channel modeling in the previous works might be inaccurate. To address this, [10] proposes a highly complicated channel model to follow closely the spatial correlation of the Jake's model. Using this channel model, they highlight that FAS has limited performance gain as N increases. Yet, the key reasons that limit the performance of FAS remain ambiguous. This is because the eigenvalue and eigenvector entries that are used in the analytical PDF/CDF expressions provide limited insights.

It is important to highlight that deriving the PDF/CDF of FAS channels is extremely challenging [10]. This is because the channels of FAS are strongly correlated and thus they have to be formulated in terms of multivariate correlated Rayleigh distributions. Over the past few decades, extensive efforts have been dedicated to this problem [17]. However, most of the

¹Throughout this paper, we refer to an active RF-chain as the RF-chain used for communications. In contrast, the term RF-chains refers to a collection of RF-chains that are connected to each antenna for it to work as intended.

works only obtain the bivariate [18], [19], trivariate [18], [20], [21], or quadvariate [21], [22] distributions while other works restrict the correlation matrix to certain forms (e.g., equally correlated [23] and exponentially correlated [24]). Fortunately, the multivariate PDF/CDF of arbitrarily correlated Rayleigh distributions are recently derived in [25]–[27]. Nevertheless, the assumption of non-singular correlation matrix is retained. In this paper, we omit this assumption (i.e., our correlation matrix could be near-singular) and address the computation problem via a suboptimal approximation.²

In addition to the above works, [29] develops a port selection algorithm that can approach the performance of optimal FAS when only the received SNR of a few ports are observed. Furthermore, [30] considers a field-response channel model while omitting the spatial correlation effect and [31] extends the model to a MIMO scenario. Moreover, FAMA can be categorized into i) slow-FAMA and ii) fast-FAMA. The earlier switches its port when the channel changes [32] while the latter switches its port on a symbol-by-symbol basis [33]. The analytical outage probability of two-user FAMA is also derived in [34].

Motivated by the aforementioned works, this paper aims to understand the fundamental limits of FAS as well as the key factors that affect its performance. To this end, we approximate the outage probability and diversity gain of FAS in closed-form expressions via a simple and accurate channel model that follows closely the spatial correlation of Jake's model. In addition, we propose a suboptimal FAS with N^* ports as well as an algorithm to approximate N^* . The main contributions of our paper are summarized as follows:

- We employ a simple and accurate channel model that follows the spatial correlation of Jake's model. Based on this channel model, we approximate the outage probability in closed-form expressions. By applying Taylor series approximation, we simplify the outage probability at high SNR into a simpler and more meaningful expression. Using this result, we obtain the diversity gain of FAS.
- We propose a suboptimal FAS with N^* ports. The proposed suboptimal FAS plays an important role as it enables FAS to achieve near-optimal performance with minimal number of ports. In particular, one may define ε_{tol} to adjust the sub-optimality of the proposed FAS.

²The computational problem of a near-singular correlation matrix is much harder to address than that of a singular matrix. This is because we can obtain an independent matrix from a singular matrix by removing the dependent entries [28]. But in the near-singular case, this approach cannot be applied. Instead, we need to rely on approximations.

For example, if ε_{tol} is small, the proposed FAS is quantifiably near-optimal at a cost of more ports. In addition, we develop a polynomial-time algorithm to approximate N^* . Besides, N^* can be used to address the near-singular correlation matrix problem.

- We provide analytical and simulation results to demonstrate the key parameters that affect the performance of FAS. Our discussions include intuitive insights on the system characteristics as well as practical guidelines for efficient FAS design.

The rest of the paper is organized as follows: Section II details the system model and performance metrics. Section III presents the outage probability and diversity gain of FAS. The details of suboptimal FAS and the algorithm to approximate N^* are discussed in Section IV. Section V provides our simulation results and we conclude the paper in Section VI.

Notations: Scalar variables are denoted by italic letters (e.g., c), vectors are denoted by boldface italic small letters (e.g., \mathbf{c}) and matrices are denoted by boldface italic capital letters (e.g., \mathbf{C}). Besides, $(\cdot)^T$ denotes transpose, $(\cdot)^H$ denotes conjugate transpose, $(\cdot)^{-1}$ denotes inverse of a matrix while $|\cdot|$ and $\|\cdot\|_F$ denotes absolute and Frobenius norm, respectively. Throughout this paper, $\log(\cdot)$ denotes logarithm with base 2, $\mathbb{E}[\cdot]$ denotes the expectation and $\mathbb{P}\{\cdot\}$ denotes the probability of an event. In addition, $f_c(\cdot)$ denotes the PDF of c , and $F_c(\cdot)$ denotes the CDF of c . The notation $\mathbf{1}_c\{\cdot\}$ is an indication function for condition c and $[\cdot]_c^{+/-}$ outputs the argument that is lower/upper bounded by c . To help readers with our mathematical content, the meanings of the key variables are explained in Table I.

II. SYSTEM MODEL

In this paper, we consider a point-to-point FAS where the transmitter is equipped with a conventional antenna and the receiver is equipped with a fluid antenna. The fluid antenna consists of one RF-chain and N preset locations (also known as ports), which are evenly distributed along a linear dimension of length $W\lambda$ where λ is the wavelength of the carrier frequency. Since the ports are closely packed together, there is a strong spatial correlation among them. Based on Jake's model [35], the spatial correlation between the m -th and n -th ports is given by

$$J_{m,n} = \sigma^2 J_0 \left(2\pi \frac{(m-n)}{N-1} W \right), \quad (1)$$

where σ^2 accounts for the large-scale fading effect and $J_0(\cdot)$ is the zero-order Bessel function of the first kind.

Table I: The meanings of key variables

Notation	Meaning
D_{FAS}	Diversity gain of FAS
h_n	Complex channel coefficient of the n -th port
\hat{h}_n	Approximation of h_n
$ h_{\text{FAS}} $	Maximum signal envelope of FAS
$J_{m,n}$	Spatial correlation between the m -th and n -th ports
\mathbf{J}	Spatial correlation matrix
\mathbf{J}'	Spatial correlation matrix with $N \rightarrow \infty$
\mathbf{K}	Co-factor of \mathbf{J}
λ	Wavelength of the carrier frequency
N	Total number of ports
N'	Rank of \mathbf{J}'
q	Minimum required rate
SNR	Transmit SNR
W	Length of the fluid antenna in terms of λ
Θ	Instantaneous received SNR of the receiver

For ease of analysis, we introduce the correlation matrix \mathbf{J} where

$$\mathbf{J} = \begin{bmatrix} J_{1,1} & \cdots & J_{1,N} \\ \vdots & \ddots & \vdots \\ J_{N,1} & \cdots & J_{N,N} \end{bmatrix}. \quad (2)$$

In (2), we have $J_{m,n} = J_{n,m}$. Therefore, using eigenvalue decomposition, we can obtain $\mathbf{J} = \mathbf{U}\Lambda\mathbf{U}^H$ where \mathbf{U} is an $N \times N$ matrix whose n -th column (denoted by \mathbf{u}_n) is the eigenvector of \mathbf{J} and $\Lambda = \text{diag}(\lambda_1, \dots, \lambda_N)$ is an $N \times N$ diagonal matrix whose n -th diagonal entry is the corresponding eigenvalue of \mathbf{u}_n . Without loss of generality, we assume that the values of the eigenvalues in Λ are arranged in descending order. i.e., $\lambda_1 \geq \dots \geq \lambda_N$.

Throughout this paper, we assume there is only one RF-chain in FAS and thus only one port can be activated for communications. The received signal of the n -th port is expressed as

$$y_n = h_n x + w_n, \quad n = 1, \dots, N, \quad (3)$$

where h_n is the complex channel coefficient of the n -th port, x is the information signal with $\mathbb{E}[|x|^2] = P$ and w_n is the additive white Gaussian noise of the n -th port with zero mean and

variance of N_0 . Due to the spatial correlation of the ports, h_n can be modeled as

$$h_n = \sum_{m=1}^N u_{n,m} \sqrt{\lambda_m} z_m, \quad (4)$$

where $u_{n,m}$ is the (n, m) -th entry of \mathbf{U} , $z_m = a_m + jb_m$, where $a_m, b_m, \forall m$, are independent and identically distributed (i.i.d.) Gaussian random variables with zero mean and variance of $\frac{1}{2}$.

According to [10], (4) can also be approximated as

$$\hat{h}_n = \Psi v_n + \sum_{m=1}^{\epsilon\text{-rank}} u_{n,m} \sqrt{\lambda_m} z_m, \quad (5)$$

where ϵ -rank is a modeling parameter, $\Psi = \sqrt{\sigma^2 - \sum_{m=1}^{\epsilon\text{-rank}} u_{n,m}^2 \lambda_m}$, $v_n = c_n + jd_n$ and $c_n, d_n, \forall n$, are i.i.d. Gaussian random variables with zero mean and variance of $\frac{1}{2}$.

To obtain the global optimum performance, FAS activates a port with the maximum signal envelope [7],³ i.e.,

$$|h_{\text{FAS}}| = \max \{|h_1|, \dots, |h_N|\}. \quad (6)$$

The instantaneous received SNR of the receiver is found as

$$\Theta = |h_{\text{FAS}}|^2 \frac{P}{N_0} = |h_{\text{FAS}}|^2 \text{SNR}, \quad (7)$$

where $\text{SNR} = \frac{P}{N_0}$ is the transmit SNR and its outage probability is defined as

$$\mathbb{P}\{\log(1 + \Theta) < q\} = \mathbb{P}\{|h_{\text{FAS}}| < \Omega\}, \quad (8)$$

where $\Omega = \sqrt{\frac{2^q - 1}{\text{SNR}}}$ and q is the minimum required rate. In addition, the diversity gain of FAS can be defined as [36]

$$\lim_{\text{SNR} \rightarrow \infty} -\frac{\log \mathbb{P}_e(\text{SNR})}{\log(\text{SNR})} \stackrel{(a)}{=} \lim_{\text{SNR} \rightarrow \infty} -\frac{\log \mathbb{P}\{\log(1 + |h_{\text{FAS}}|^2 \text{SNR}) < q\}}{\log(\text{SNR})} = D_{\text{FAS}}, \quad (9)$$

where (a) follows from the fact that error probability and outage probability differ by a constant shift at high SNR [37].

³Due to the port spatial correlation, it is shown in [32] that only a small number of observed ports/training is required to obtain the full channel state information.

III. OUTAGE PROBABILITY AND DIVERSITY GAIN OF FAS

As it is seen in (4), the complex channel coefficients $\mathbf{h} = [h_1, \dots, h_N]^T$ are correlated. Therefore, $|\mathbf{h}|$ is a correlated Rayleigh random vector. We present the following lemmas to obtain the closed-form outage probability and diversity gain of FAS.

Lemma 1. *The PDF of $|\mathbf{h}|$ can be approximated as*

$$\begin{aligned} & f_{|\mathbf{h}|}(|h_1|, \dots, |h_N|) \\ & \approx \eta \sum_{s_1=0}^{s_0} \sum_{s_2=0}^{s_1} \dots \sum_{s_T=0}^{s_{T-1}} \left(\frac{1}{2}\right)^{\sum_{t=1}^T s_t^*} \prod_{t=1}^T \beta(t, s_t^*) \sum_{\mathbf{v} \in \mathcal{V}} \left[\prod_{t=1}^T \begin{pmatrix} s_t^* \\ v_t \end{pmatrix} \right] \left[(2\pi)^N \prod_{i=1}^N \mathbf{1}_{\{\Delta_i=0\}} \right]. \end{aligned} \quad (10)$$

Proof: See Appendix A. ■

In (10), $\eta = \frac{\prod_{n=1}^N |h_n|}{\pi^N \det(\mathbf{J})} \exp \left\{ -\frac{\sum_{n=1}^N |h_n|^2 K_{n,n}}{\det(\mathbf{J})} \right\}$, $T = \frac{N(N-1)}{2}$, $\beta(t, s_t^*) \triangleq \frac{\zeta_t^{s_t^*}}{s_t^*!}$, $\zeta_t = -\frac{2K_{m,n}|h_n||h_m|}{\det(\mathbf{J})}$ and $s_t^* = s_t - s_{t+1}$ with $s_{T+1} = 0$. Throughout this paper, the subscript t and m, n are related as follows: $t = n + (m-1)N - \frac{m(m+1)}{2}$, $m < n$, while m, n can be obtained from t with $m = \min m' \in \mathbb{Z}$ subject to $\sum_{i=1}^{m'} (N-i) > t$ and $n = t - (m-1)N + \frac{m(m+1)}{2}$.

Note that s_0 is a finite constant which has to be large for the approximation to be accurate. In addition, $\mathbf{v} = [v_1, \dots, v_T]^T$, \mathcal{V} denotes the set of all the possible permutations and $\Delta_i = \sum_{n=1}^N G_{i,n} - \sum_{n=1}^N G_{n,i} - G_{i,i}$. Furthermore, $K_{m,n}$ is the (m, n) -th entry of \mathbf{K} where \mathbf{K} is the co-factor of \mathbf{J} , and $G_{m,n}$ is the (m, n) -th entry of \mathbf{G} where \mathbf{G} is defined as

$$\mathbf{G} = \begin{bmatrix} 0 & \gamma_1 & \gamma_2 & \cdots & \gamma_{N-1} \\ & \gamma_N & \cdots & & \gamma_{2N-3} \\ \vdots & \ddots & & & \vdots \\ & & & & \gamma_T \\ 0 & \cdots & & & 0 \end{bmatrix}, \quad (11)$$

and $\gamma_t = 2v_t - s_t^* \in \mathbb{Z}$.

Lemma 2. *The CDF of $|\mathbf{h}|$ can be approximated as*

$$\begin{aligned} F_{|\mathbf{h}|}(R_1, \dots, R_N) & \approx \sum_{s_1=0}^{s_0} \sum_{s_2=0}^{s_1} \dots \sum_{s_T=0}^{s_{T-1}} \frac{g(\mathbf{s}^*)}{\pi^N \det(\mathbf{J})} \prod_{t=1}^T \frac{(-K_{m,n})^{s_t^*}}{s_t^*! \det(\mathbf{J})^{s_t^*}} \times \\ & \prod_{n=1}^N \frac{1}{2} \left(\frac{K_{n,n}}{\det(\mathbf{J})} \right)^{-\frac{s_n}{2} - \frac{1}{2}} \left[\Gamma \left(\frac{1+\bar{s}_n}{2} \right) - \Gamma \left(\frac{1+\bar{s}_n}{2}, \frac{K_{n,n} R_n^2}{\det(\mathbf{J})} \right) \right]. \end{aligned} \quad (12)$$

Proof: See Appendix B. ■

In (12), we have $\bar{s}_n = \sum_{i=1}^N S_{i,n}^* + \sum_{i=1}^{n-1} S_{i,n}^* + 1$ where $S_{i,n}^*$ is the (i, n) -th entry of \mathbf{S}^* and \mathbf{S}^* is introduced in (36). Furthermore,

$$g(\mathbf{s}^*) = \left(\frac{1}{2}\right)^{\sum_{t=1}^T s_t^*} \sum_{\mathbf{v} \in \mathcal{V}} \left[\prod_{t=1}^T \begin{pmatrix} s_t^* \\ v_t \end{pmatrix} \right] (2\pi)^N \prod_{i=1}^N \mathbf{1}_{\{\Delta_i=0\}}. \quad (13)$$

The expressions in (10) and (12) are extremely complicated. Nevertheless, they enable us to obtain more insightful derivations as shown later in this paper. Using the above lemmas, we present the following theorems.

Theorem 1. *The outage probability of FAS can be approximated in a closed-form expression as*

$$\begin{aligned} \mathbb{P}\{|h_{FAS}| < \Omega\} &= F_{|\mathbf{h}|}(\Omega, \dots, \Omega) \\ &\approx \sum_{s_1=0}^{s_0} \sum_{s_2=0}^{s_1} \dots \sum_{s_T=0}^{s_{T-1}} \frac{g(\mathbf{s}^*)}{\pi^N \det(\mathbf{J})} \prod_{t=1}^T \frac{(-K_{m,n})^{s_t^*}}{s_t^*! \det(\mathbf{J})^{s_t^*}} \times \\ &\quad \prod_{n=1}^N \frac{1}{2} \left(\frac{K_{n,n}}{\det(\mathbf{J})} \right)^{-\frac{\bar{s}_n}{2} - \frac{1}{2}} \left[\Gamma\left(\frac{1+\bar{s}_n}{2}\right) - \Gamma\left(\frac{1+\bar{s}_n}{2}, \frac{K_{n,n}\Omega^2}{\det(\mathbf{J})}\right) \right]. \end{aligned} \quad (14)$$

Proof: The result can be obtained using Lemma 2 and substituting $R_1 = \dots = R_N = \Omega$. ■

Remark 1. According to [10], \mathbf{h} can be modeled using $\hat{\mathbf{h}} = [\hat{h}_1, \dots, \hat{h}_N]^T$ and using the latter model, they show that the outage probability of FAS can be approximated by

$$F_{|h_{FAS}|}(\Omega) \approx \left[\prod_{n=1}^N \int_0^\infty \frac{1}{\sum_{m=1}^{\text{rank}} u_{n,m}^2 \lambda_m} \exp\left(-\frac{r}{\sum_{m=1}^{\text{rank}} u_{n,m}^2 \lambda_m}\right) \left(1 - Q_1\left(\frac{\sqrt{2r}}{\Psi}, \frac{\sqrt{2}\Omega}{\Psi}\right)\right)^L dr \right]^{\frac{1}{L}}, \quad (15)$$

where $Q_1(\cdot, \cdot)$ is the Marcum-Q function and $L = \min\left\{\frac{1.52(N-1)}{2\pi W}, N\right\}$. Note that (15) is a remarkable expression as each n term only has a single integral. Nevertheless, we found that it is challenging to obtain deeper insights from this expression.

Theorem 2. *The outage probability of FAS at high SNR is given by*

$$\mathbb{P}\{|h_{FAS}| < \Omega\} = \frac{1}{\det(\mathbf{J})} \Omega^{2N} + o\left(\frac{1}{SNR^N}\right). \quad (16)$$

Proof: See Appendix C. ■

Theorem 3. *The diversity gain of FAS is approximately expressed as*

$$D_{FAS} \approx \min\{N, N'\}, \quad (17)$$

where N' is the numerical rank of \mathbf{J}' such that \mathbf{J}' is the covariance matrix as defined in (2) with $N \rightarrow \infty$ for a fixed W .

Proof: See Appendix D. ■

In Theorem 2, we can interpret $\det(\mathbf{J}^{-1})$ as the penalty term and Ω^2 as gain of FAS that scales exponentially w.r.t. N . Meanwhile, the term with little-o can be ignored as it approaches zero if the SNR is high. Nevertheless, in Theorem 3, we can see that the diversity gain is limited by $\min\{N, N'\}$. Thus, increasing N over N' might not be useful. Notice that these interpretations cannot be directly obtained from (15).

IV. SUBOPTIMAL SOLUTION: FAS WITH N^* PORTS

At a fundamental level, [11] showed that increasing the number of channels (or ports) would yield a diminishing gain (i.e., the average received SNR gain is $\sum_n^N \frac{1}{n}$). In fact, [10] showed that for a fixed W , the outage probability of FAS might remain similar after some N . For ease of expositions, we denote this N as N^* where $N^* \leq N$.

To the best of our knowledge, little is known about N^* . In fact, it is very challenging to obtain N^* as it varies with the parameter W or more precisely the correlation matrix \mathbf{J} .⁴ Yet, finding N^* is essential in both theory and practice since it helps FAS to achieve an efficient performance with a minimal number of ports. In this section, we present a simple method to approximate N^* for a given W .

To begin with, we present the following theorem.

Theorem 4. Suppose the channels of FAS with N ports are denoted by \mathbf{h} . Then \mathbf{h} can be well-approximated by $\tilde{\mathbf{h}} = [\tilde{h}_1, \dots, \tilde{h}_{\tilde{N}}]^T$ where

$$\tilde{h}_n = \sum_{m=1}^{\tilde{N}} u_{n,m} \sqrt{\lambda_m} z_m, \quad (18)$$

where \tilde{N} is the numerical rank of \mathbf{J} . That is, the PDF and CDF of \mathbf{h} and $\tilde{\mathbf{h}}$ are similar.

Proof: Let \tilde{N} be the numerical rank of \mathbf{J} where $\tilde{N} \leq N$. Using the definition of numerical rank, we have $\lambda_n < \epsilon$ for $n \in \{\tilde{N} + 1, \dots, N\}$ where $\epsilon \approx 0$. According to Eckart-Young-Mirsky

⁴Referring to (1) and (2), we can see that N^* depends on the parameter W .

theorem [38], the optimal $\tilde{\mathbf{J}}$ that minimizes the Frobenius norm between matrix \mathbf{J} and $\tilde{\mathbf{J}}$ subject to the constraint that $\text{rank}(\tilde{\mathbf{J}}) \leq \tilde{N}$ is $\tilde{\mathbf{J}} = \mathbf{U}\tilde{\Lambda}\mathbf{U}^H$ where $\tilde{\Lambda} = \text{diag}(\lambda_1, \dots, \lambda_{\tilde{N}}, 0, \dots 0)$.

Using this insight, we introduce $\tilde{\mathbf{h}}$ as defined in Theorem 4 where the covariance of $\tilde{\mathbf{h}}$ is $\tilde{\mathbf{J}}$ (i.e., the best approximation of \mathbf{J} for $\text{rank}(\tilde{\mathbf{J}}) \leq \tilde{N}$). As a result, we can well-approximate \mathbf{h} using $\tilde{\mathbf{h}}$ since the Frechet distance between the two distributions is [39]

$$\begin{aligned} W_2 \left(\mathcal{CN}(0_{N \times 1}, \mathbf{J}), \mathcal{CN}(0_{N \times 1}, \tilde{\mathbf{J}}) \right) &= \left\| (\Lambda)^{\frac{1}{2}} - (\tilde{\Lambda})^{\frac{1}{2}} \right\|_F^2 \\ &\approx 0. \end{aligned} \quad (19)$$

■

Corollary 1. *If we have the exact eigenvalues and rank of \mathbf{J} , then $\mathbf{h} = \tilde{\mathbf{h}}$.*

Proof: Let Λ and \tilde{N} be the exact eigenvalues and rank of \mathbf{J} . Using the definition of rank, we have $\lambda_n = 0$ for $n \in \{\tilde{N} + 1, \dots, N\}$. It then follows that the Frechet distance between the distributions of \mathbf{h} and $\tilde{\mathbf{h}}$ is zero. ■

As seen in (19), it is the eigenvalues of correlation matrix that play a critical role in the channel approximation. Motivated by this insight, we introduce a new formula as follows:

$$\begin{aligned} \varepsilon_{N^*} &= S_N - S_{N^*} \\ &= \sigma^2 - S_{N^*}, \end{aligned} \quad (20)$$

where $S_{N^*} = \frac{1}{N} \sum_{n=1}^{N^*} \lambda_n$. Note that (20) is analogous to (19) in the sense that the left hand side of (20) measures the gap between the distributions of \mathbf{h} and \mathbf{h}^* , where \mathbf{h}^* is similarly defined as in (18) but we instead replace \tilde{N} with N^* and impose that $N^* \leq \tilde{N}$. Meanwhile, on the right hand side of (20), we consider the average eigenvalues of \mathbf{J}^* , where \mathbf{J}^* is the covariance of \mathbf{h}^* .

To reduce the number of required ports, we define $\varepsilon_{\text{tol}} > 0$ and find the smallest integer N^* such that $\varepsilon_{\text{tol}} \geq \varepsilon_{N^*}$. Since \mathbf{J}^* only has N^* dominant eigenvalues, we propose to employ a suboptimal FAS with N^* ports. Interestingly, ε_{tol} has a nice heuristic interpretation in practice. Specifically, it defines the sub-optimality of the proposed FAS, i.e., the proposed FAS is near optimal if ε_{tol} is small and less optimal if ε_{tol} is large.

By fixing ε_{tol} appropriately,⁵ we observe that FAS with N^* ports yields considerable improvement over all FAS with $N < N^*$ ports while most of the FAS with $N > N^*$ ports yields

⁵We recommend to set $\varepsilon_{\text{tol}} = 0.01\sigma^2$ (i.e., the average eigenvalues of \mathbf{J}^* is 99% of that of \mathbf{J})

Algorithm 1 Method of approximating N^* given W

```

1: Input:  $W, \varepsilon_{\text{tol}}$ ; Output:  $N^*$ 
2: Compute  $\mathbf{J} = \mathbf{U}\Lambda\mathbf{U}^H$ 
3: Define  $n = 1$  and compute  $\varepsilon_n$ 
4: While  $\varepsilon_{\text{tol}} < \varepsilon_n$  and  $n < \tilde{N}$ 
5:    $n = n + 1$ 
6:    $\varepsilon_n = \sigma^2 - S_n$ 
7: end
8: Return  $n$  as  $N^*$ 

```

marginal improvement over FAS with $N - 1$ ports. Note that we usually have $N^* < \tilde{N}$ if \mathbf{J} is ill-conditioned and $N^* = \tilde{N}$ if \mathbf{J} is well-conditioned.

The method of approximating N^* is given in Algorithm 1. To measure the computational complexity of our algorithm, we consider the floating-point operations (flops). A flop is defined as one addition, subtraction, multiplication or division of two floating point numbers [40]. In Algorithm 1, computing \mathbf{J} and $\mathbf{U}\Lambda\mathbf{U}^H$ requires $6N^2$ and $21N^3$ flops, respectively [41]. Computing ε_n requires $n + 1$ flops for each n . Therefore, the total flops of Algorithm 1 is $21N^3 + 6N^2 + \frac{1}{2}N^{*2} + \frac{3}{2}N^*$, which has a polynomial time-complexity of $\mathcal{O}(N^3)$ since $N^* \leq N$. In other words, Algorithm 1 is only dominated by the computation of $\mathbf{U}\Lambda\mathbf{U}^H$.

Note that N^* is also useful in theory. For example, Lemma 1 and 2 and Theorem 1, 2, and 3 are incalculable if \mathbf{J} is near-singular. To address this, we present the following theorem.

Theorem 5. *If \mathbf{J} is near-singular, then we can approximate the channels of FAS with N ports using N^* ports from a computational perspective. Nevertheless, a small gap between the channel distributions of FAS with N ports and that of N^* ports might exist.*

Proof: If \mathbf{J} is near-singular, then one or more entries are almost linear combinations of the other entries. Thus, we can remove these nearly-dependent entries and only consider N^* independent entries. Since FAS with N^* ports has N^* dominant eigenvalues, Lemma 1 and 2 and Theorem 1, 2, and 3 are calculable. Nevertheless, there might be a small gap between the channel distributions of FAS with N ports and that of N^* ports since the entries are nearly-dependent only. ■

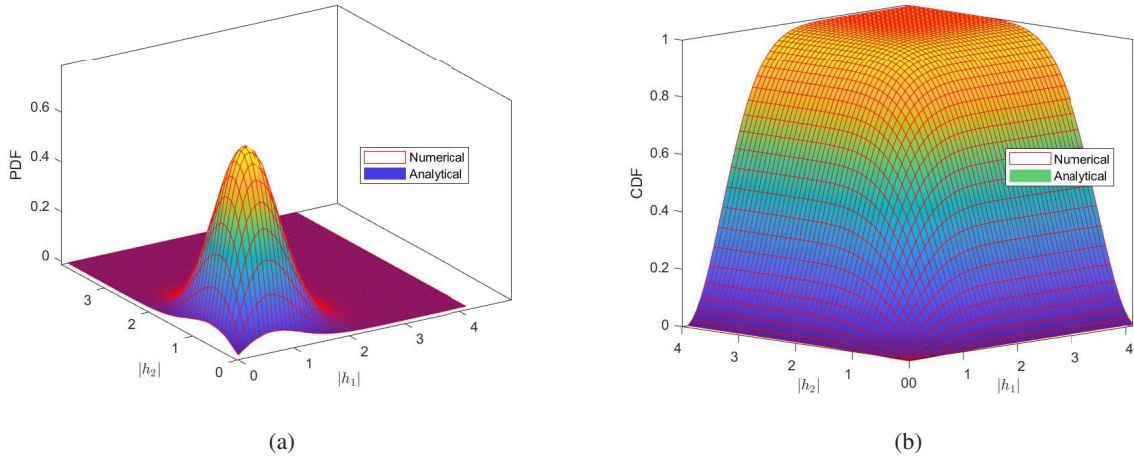


Figure 1: FAS with 2 ports: a) joint PDF; b) joint CDF.

V. RESULTS AND DISCUSSIONS

In this section, we present simulation results to better understand the performance of FAS. We focus on the design of an efficient FAS as well as the factors that limit its performance. Unless stated otherwise, we assume that $\sigma^2 = 1$, $N = 50$, $W = 0.5$, $q = 10$ and $SNR = 30$ dB.

Firstly, we demonstrate the accuracy of (10) and (12). In order to visualize the joint PDF and CDF of $|\mathbf{h}|$, we consider a FAS with 2 ports (i.e., $N = 2$). In Fig. 1, the red grid represents the numerical PDF/CDF while the solid surface is the analytical PDF/CDF. As observed, the approximation of the PDF/CDF of $|\mathbf{h}|$ matches closely with the numerical ones over all the distributed region. Still, it is worth noting that (10) and (12) are very complicated. Thus, approximations with simpler expressions remain desirable.

Fig. 2 compares the outage probability of FAS to (14) and (15). As observed, (14) is more accurate because the analytical expression is derived directly from the multivariate correlated Rayleigh distributions and the approximation is only used when truncating the infinite series to a finite one. Here, we assume that $s_0 = 20$. Compared to the numerical result, the truncation error is negligible as long as s_0 is sufficiently large. In contrast, (15) is less accurate because the outage probability of FAS is approximated using the power of single integrals where such simplification may lead to some inaccuracies. Nevertheless, it is worth highlighting that (14) can only be computed for small N as its expression is highly complicated. Thus, (15) is still useful for large N .

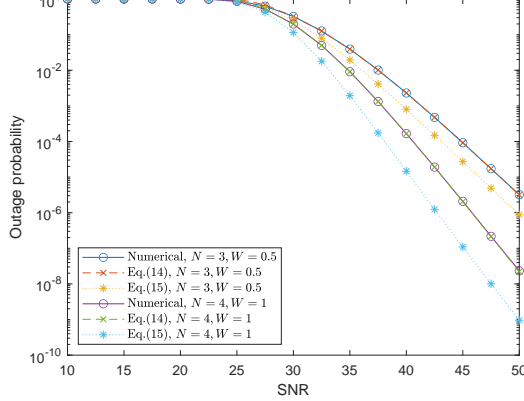


Figure 2: Outage probability of FAS versus SNR.

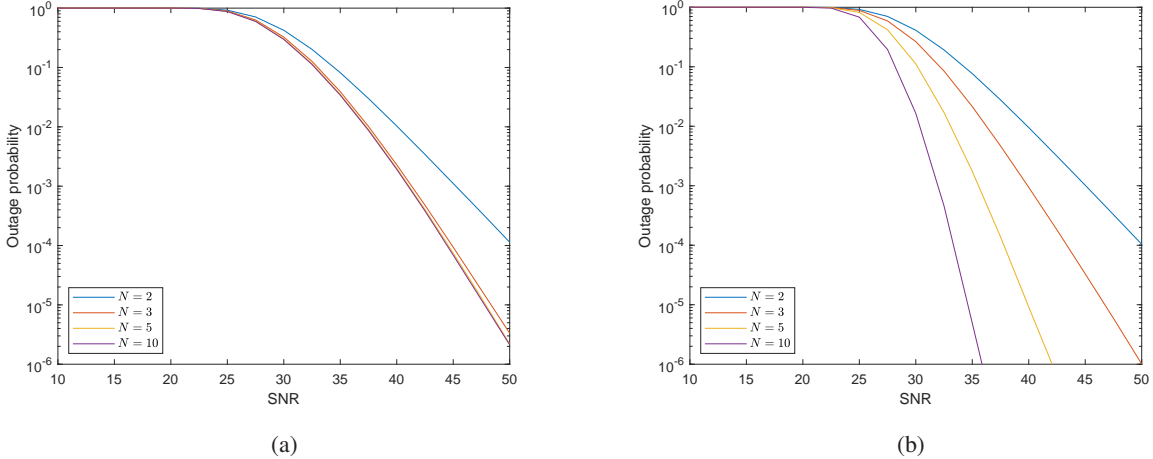


Figure 3: Outage probability of FAS versus SNR for different N and W : a) $W = 0.5$; b) $W = 10$.

In Fig. 3, we compute the outage probability of FAS versus SNR for different N and W . Comparing Fig. 3(a) and Fig. 3(b), we can clearly see that the outage probability is mainly limited by W . In particular, if W is small and N is large, the outage probability remains similar which is in alignment with the findings of [10]. Nevertheless, if W is sufficiently large, the outage probability decreases significantly as N increases.

To better understand this, we further compare the outage probability of FAS to (15) and (16) in Fig. 4. Compared to the numerical result, we can see that (15) is less accurate while (16) is accurate as SNR increases. Specifically, (16) is much more accurate as SNR increases because we apply Taylor series approximation at around zero which corresponds to asymptotically high

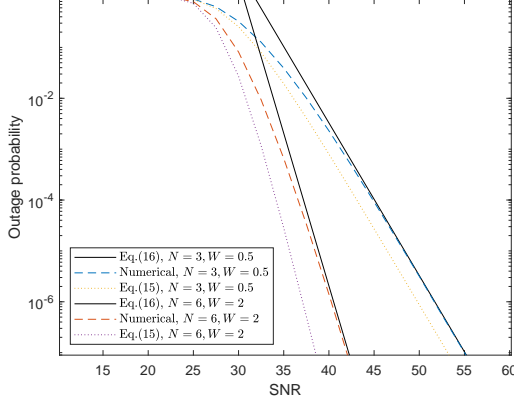


Figure 4: Outage probability of FAS at high SNR.

SNR. Hence, the error becomes negligible at high SNR. From (16), we learn that $\det(\mathbf{J}^{-1})$ plays a critical role in the performance of FAS. In particular, \mathbf{J} has to be well-conditioned in order for Ω^{2N} to be the dominant term. If \mathbf{J} is near-singular, then N is no longer important. This is because $\det(\mathbf{J}^{-1})$ cannot be compensated by Ω^{2N} . To make \mathbf{J} a well-conditioned matrix, we can either increase W for a fixed N or decrease N for a fixed W . Nevertheless, we believe that larger N does not cause any harm to the system in practice. It only makes the theoretical analysis harder.

As shown in Fig. 5(a), we compare the outage probability of FAS with N ports and that of N' ports for different W where $N < N'$. As it is seen, the outage probability of the earlier is lower bounded by the latter regardless of W . In Fig. 5(b), we investigate the opposite case where $N > N'$. As observed, the outage probability of FAS with N ports and that of N' ports are the same for different W . Thus, the diversity gain of FAS is limited by $\min\{N, N'\}$, which verifies Theorem 3. Theorem 3 also suggests that increasing the ports beyond N' provides no improvement in a point-to-point setting.

Fig. 6(a) presents the CDF of \mathbf{h} and $\tilde{\mathbf{h}}$ where we fix $R_1 = \dots = R_N = R$. In the result, no significant variation is observed between \mathbf{h} and $\tilde{\mathbf{h}}$ regardless of R , N and W . This is because the Frechet distance between the two distributions is always near zero. This confirms Theorem 4 and suggests that one can always use $\tilde{\mathbf{h}}$ instead of \mathbf{h} . In addition, Fig. 6(b) shows the CDF of \mathbf{h} and \mathbf{h}^* . Unlike the previous result, there is a small gap between the two distributions as W increases. Despite having some gaps, the approximation is still fairly good. This result verifies

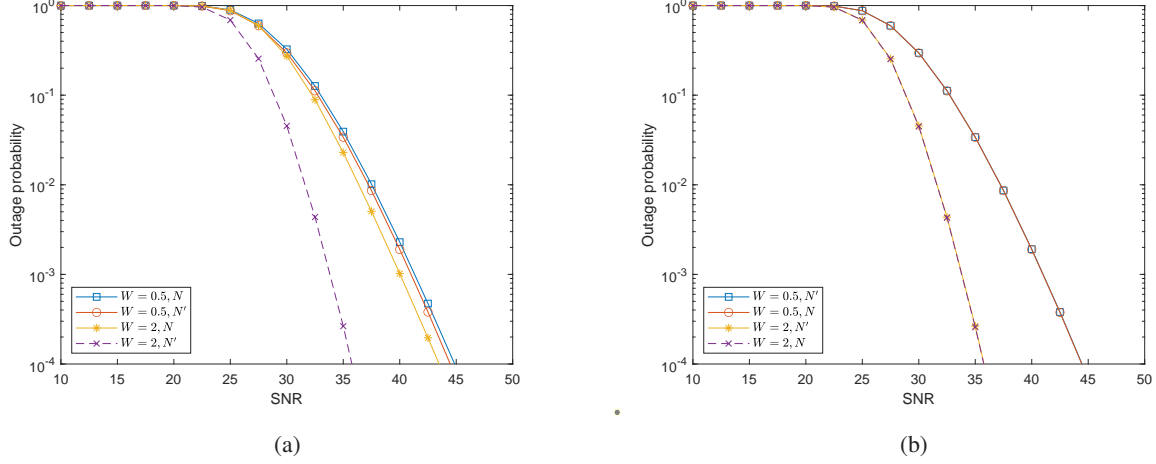


Figure 5: Outage probability of FAS with N ports versus N' ports: a) $N = 3 < N'$; b) $N = 50 > N'$.

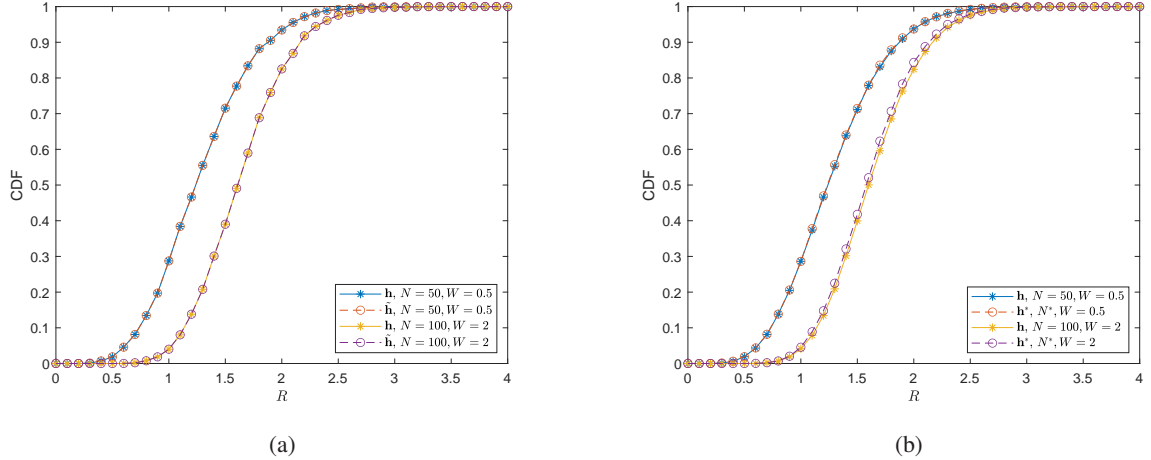


Figure 6: CDF between: a) \mathbf{h} and $\tilde{\mathbf{h}}$; b) \mathbf{h} and \mathbf{h}^* .

Theorem 5.

Next, we investigate the accuracy of Algorithm 1 and the efficiency of the proposed suboptimal FAS. The parameter N^* for different W using Algorithm 1 is summarized in Table II. As seen in Fig. 7, the outage probability of FAS with N^* ports is promising. Specifically, FAS with N^* ports yields a significant improvement over FAS with $N^* - 1$ ports. Meanwhile, FAS with $N + 1$ ports provides negligible improvement over FAS with N^* ports. Thus, we may use the

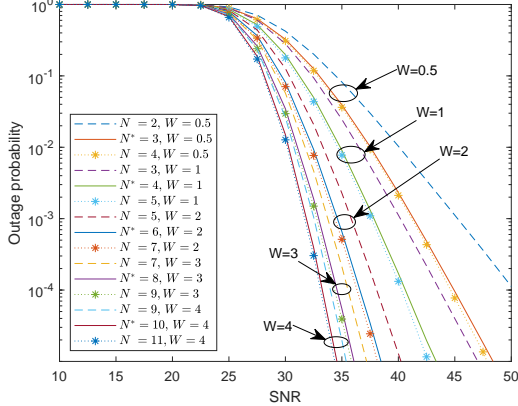


Figure 7: Outage probability of suboptimal FAS.

Table II: Parameter N^* for different W using algorithm 1 where $\varepsilon_{\text{tol}} = 0.01$

W	0.5	1	2	3	4
N^*	3	4	6	8	10

suboptimal FAS for an efficient performance.

Finally in Fig. 8, we compare the outage probability of the proposed suboptimal FAS, the optimal FAS, the single antenna (SISO) system, the N -branch SC system, and the N -branch MRC system. In SC and MRC systems, we assume there are N RF-chains where each antenna has to be at least $\frac{\lambda}{2}$ apart and their spatial correlations are considered. Note that MRC has N active RF-chains. Results show that the proposed suboptimal FAS outperforms SISO and SC systems. This improvement is due to the ability of FAS switching to the best port within a finite W .

In addition, MRC has the lowest outage probability and it outperforms optimal FAS. This superiority is due to the power gain where a larger number of active RF-chains (i.e., $\lfloor \frac{W}{0.5} \rfloor + 1$) is utilized in MRC while FAS has only one active RF-chain. Although MRC is more superior than the suboptimal FAS, the latter can achieve a similar performance as compared to the earlier when $W = 0.5$. Yet, it is important to recall that MRC has one additional RF-chain as compared to the suboptimal FAS in this case. Thus, it will be very interesting to compare the performance of MIMO-FAS and MIMO with the same number of active RF-chains.

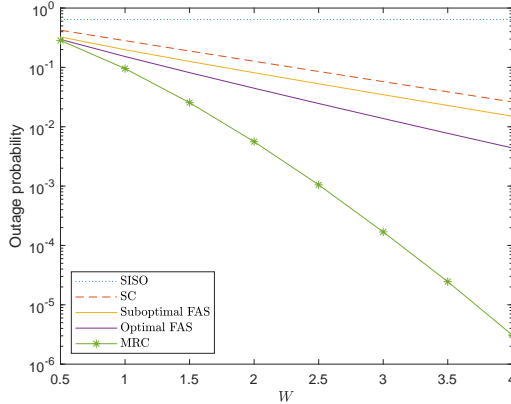


Figure 8: Outage probability of suboptimal FAS vs. SISO, SC, and MRC.

VI. CONCLUSIONS

In this paper, we considered FAS and approximated its outage probability and diversity gain in closed-form expressions. New meaningful insights were obtained from the analytical results, and simulation results were given to better understand the factors that limit the performance of FAS. Our results showed that the performance of FAS strongly depends on the spatial correlation matrix \mathbf{J} . Specifically, increasing the ports beyond N' yields no diversity gain in a point-to-point setting. Instead, increasing N causes the correlation matrix \mathbf{J} to be ill-conditioned. To address this, one can either increase W for a fixed N or decrease N for a fixed W . In addition, we proposed a suboptimal FAS with N^* ports. By fixing an appropriate ε_{tol} , the proposed scheme enabled us to obtain a significant gain over FAS with $N^* - 1$ while it nearly achieved the same performance as FAS with $N^* + 1$ ports. Thus, the approximation of N^* is useful since a larger number of ports yields diminishing gains and additional costs. Furthermore, N^* can be used to approximate the channels of FAS with N ports if the correlation matrix \mathbf{J} is near-singular. Last but not least, the proposed suboptimal FAS outperforms SISO and SC systems but falls behind MRC due to having a single active RF-chain. Nevertheless, it was discovered that suboptimal FAS and MRC achieve similar performance when $W = 0.5$. Thus, it would be interesting to study the performance of MIMO-FAS and MIMO in the future.

APPENDIX A: APPROXIMATED PDF OF $|\mathbf{h}|$

The exact PDF of $|\mathbf{h}|$ is first derived in [25]–[27]. In this paper, we employ similar steps and further approximate the PDF of $|\mathbf{h}|$ by introducing \mathbf{G} : an $N \times N$ matrix, using an accurate

binomial theorem, and truncating the infinite series to a finite one for ease of computation. According to [36], the PDF of a circularly symmetric complex Gaussian random variables is known as

$$f(\mathbf{h}) = \frac{1}{\pi^N \det(\mathbf{J})} \exp \left\{ -\mathbf{h}^H \mathbf{J}^{-1} \mathbf{h} \right\}, \quad (21)$$

where $\mathbf{J}^{-1} = \frac{\mathbf{K}^T}{\det(\mathbf{J})}$ via Crammer rule. Using [42, (7-8) & (7-9)], the PDF of (21) in terms of its amplitude and phase can be obtained as

$$f_{|\mathbf{h}|, \theta}(|h_1|, \theta_1, \dots, |h_N|, \theta_N) = \eta \prod_{t=1}^T \exp \left\{ \zeta_t \cos(\bar{\theta}_t) \right\}, \quad (22)$$

where $\eta = \frac{\prod_{n=1}^N |h_n|}{\pi^N \det(\mathbf{J})} \exp \left\{ -\frac{\sum_{n=1}^N |h_n|^2 K_{n,n}}{\det(\mathbf{J})} \right\}$, $T = \frac{N(N-1)}{2}$, $\zeta_t = -\frac{2K_{m,n}|h_n||h_m|}{\det(\mathbf{J})}$ and $\bar{\theta}_t = \theta_n - \theta_m$. Throughout this paper, we use the mapping function $t = n + (m-1)N - \frac{m(m+1)}{2}$, $m < n$, while (m, n) can be obtained from t by setting $m = \min m' \in \mathbb{Z}$ subject to $\sum_{i=1}^{m'} (N-i) > t$ and $n = t - (m-1)N + \frac{m(m+1)}{2}$.

Integrating (22) w.r.t. $\theta_n, \forall n$ over $[0, 2\pi]$, we have

$$\begin{aligned} & f_{|\mathbf{h}|}(|h_1|, \dots, |h_N|) \\ &= \int_0^{2\pi} \cdots \int_0^{2\pi} f(|h_1|, \theta_1, \dots, |h_N|, \theta_N) d\theta_1 \dots d\theta_N \end{aligned} \quad (23)$$

$$\stackrel{(a)}{=} \eta \int_0^{2\pi} \cdots \int_0^{2\pi} \prod_{t=1}^T \sum_{s_t=0}^{\infty} \frac{\zeta_t^{s_t}}{s_t!} \cos(\bar{\theta}_t)^{s_t} d\theta_1 \dots d\theta_N \quad (24)$$

$$\stackrel{(b)}{=} \eta \sum_{s_1=0}^{\infty} \sum_{s_2=0}^{s_1} \cdots \sum_{s_T=0}^{s_{T-1}} \prod_{t=1}^T \beta(t, s_t^*) \int_0^{2\pi} \cdots \int_0^{2\pi} \cos(\bar{\theta}_t)^{s_t^*} d\theta_1 \dots d\theta_N \quad (25)$$

$$\begin{aligned} & \stackrel{(c)}{=} \eta \sum_{s_1=0}^{\infty} \sum_{s_2=0}^{s_1} \cdots \sum_{s_T=0}^{s_{T-1}} \left(\frac{1}{2} \right)^{\sum_{t=1}^T s_t^*} \prod_{t=1}^T \beta(t, s_t^*) \times \\ & \quad \int_0^{2\pi} \cdots \int_0^{2\pi} \prod_{t=1}^T (\exp \{j\bar{\theta}_t\} + \exp \{-j\bar{\theta}_t\})^{s_t^*} d\theta_1 \dots d\theta_N \end{aligned} \quad (26)$$

$$\begin{aligned} & \stackrel{(d)}{=} \eta \sum_{s_1=0}^{\infty} \cdots \sum_{s_T=0}^{s_{T-1}} \left(\frac{1}{2} \right)^{\sum_{t=1}^T s_t^*} \prod_{t=1}^T \beta(t, s_t^*) \sum_{\mathbf{v} \in \mathcal{V}} \prod_{t=1}^T \binom{s_t^*}{v_t} \times \\ & \quad \int_0^{2\pi} \cdots \int_0^{2\pi} \exp \left\{ j \sum_{t=1}^T \gamma_t \bar{\theta}_t \right\} d\theta_1 \dots d\theta_N, \end{aligned} \quad (27)$$

where (24) is obtained by using $\exp \{x\} = \sum_{s=0}^{\infty} \frac{x^s}{s!}$ and (25) is obtained using Cauchy product of power series where $\beta(t, s_t^*) \triangleq \frac{\zeta_t^{s_t^*}}{s_t^*!}$ and $s_t^* = s_t - s_{t+1}$ with $s_{T+1} = 0$. Furthermore, (26)

is obtained using $\cos(x) = \frac{\exp(jx) + \exp(-jx)}{2}$ and (27) is obtained using binomial theorem where $\mathbf{v} = [v_1, \dots, v_T]^T$, \mathcal{V} denotes the set of all the possible permutations and $\gamma_t = 2v_t - s_t^* \in \mathbb{Z}$.

Note that $\int_0^{2\pi} \dots \int_0^{2\pi} \exp \left\{ j \sum_{t=1}^T \gamma_t \bar{\theta}_t \right\} d\theta_1 \dots d\theta_N = (2\pi)^N$ if and only if $\sum_{t=1}^T \gamma_t \bar{\theta}_t = 0$, and otherwise zero. Therefore, we introduce a new matrix \mathbf{G} as defined in (11) and the matrix $\bar{\Theta}$ given by

$$\bar{\Theta} = \begin{bmatrix} 0 & \bar{\theta}_1 & \bar{\theta}_2 & \dots & \bar{\theta}_{N-1} \\ & \bar{\theta}_N & \dots & \bar{\theta}_{2N-3} \\ \vdots & \ddots & & \vdots \\ & & \bar{\theta}_T \\ 0 & \dots & 0 \end{bmatrix} = \begin{bmatrix} 0 & \theta_2 - \theta_1 & \theta_3 - \theta_1 & \dots & \theta_N - \theta_1 \\ & \theta_3 - \theta_2 & \dots & \theta_N - \theta_2 \\ \vdots & \ddots & & \vdots \\ & & \theta_N - \theta_{N-1} \\ 0 & & \dots & & 0 \end{bmatrix}. \quad (28)$$

Using $\bar{\Theta}$ and \mathbf{G} , we can easily integrate (27) w.r.t. to θ_i by taking the sum of the same entries of \mathbf{G} as that of $\bar{\Theta}$ with θ_i , i.e., $\Delta_i = \sum_{n=1}^N G_{i,n} - \sum_{n=1}^N G_{n,i} - G_{i,i}$. Therefore, (27) leads to

$$(27) = \eta \sum_{s_1=0}^{\infty} \sum_{s_2=0}^{s_1} \dots \sum_{s_T=0}^{s_{T-1}} \left(\frac{1}{2} \right)^{\sum_{t=1}^T s_t^*} \prod_{t=1}^T \beta(t, s_t^*) \sum_{\mathbf{v} \in \mathcal{V}} \left[\prod_{t=1}^T \binom{s_t^*}{v_t} \right] \left[(2\pi)^N \prod_{i=1}^N \mathbf{1}_{\{\Delta_i=0\}} \right] \quad (29)$$

$$\stackrel{(a)}{\approx} \eta \sum_{s_1=0}^{s_0} \sum_{s_2=0}^{s_1} \dots \sum_{s_T=0}^{s_{T-1}} \left(\frac{1}{2} \right)^{\sum_{t=1}^T s_t^*} \prod_{t=1}^T \beta(t, s_t^*) \sum_{\mathbf{v} \in \mathcal{V}} \left[\prod_{t=1}^T \binom{s_t^*}{v_t} \right] \left[(2\pi)^N \prod_{i=1}^N \mathbf{1}_{\{\Delta_i=0\}} \right], \quad (30)$$

where (a) can be obtained using the facts that $\left(\frac{1}{2}\right)^{\sum_{t=1}^T s_t^*}$ is monotonically decreasing in each summation term and $\beta(t, s_t^*) \approx 0$ if s_t^* is sufficiently large.

APPENDIX B: APPROXIMATED CDF OF $|\mathbf{h}|$

Using (10), the CDF of $|\mathbf{h}|$ can be obtained as

$$F(R_1, \dots, R_N) \approx \int_0^{R_1} \dots \int_0^{R_N} f_{|\mathbf{h}|}(|h_1|, \dots, |h_N|) d|h_1| \dots d|h_N| \quad (31)$$

$$= \sum_{s_1=0}^{s_0} \sum_{s_2=0}^{s_1} \dots \sum_{s_T=0}^{s_{T-1}} \frac{g(\mathbf{s}^*)}{\pi^N \det(\mathbf{J})} \prod_{t=1}^T \frac{(-2K_{m,n})^{s_t^*}}{s_t^*! \det(\mathbf{J})^{s_t^*}} \int_0^{R_1} \dots \int_0^{R_N} \times \quad (32)$$

$$\prod_{n=1}^N |h_n| \prod_{n=1}^N \prod_{m < n} |h_n|^{s_n^*} |h_m|^{s_m^*} \exp \left\{ -\frac{\sum_{n=1}^N |h_n|^2 K_{n,n}}{\det(\mathbf{J})} \right\} d|h_1| \dots d|h_N|$$

$$= \sum_{s_1=0}^{s_0} \sum_{s_2=0}^{s_1} \dots \sum_{s_T=0}^{s_{T-1}} \frac{g(\mathbf{s}^*)}{\pi^N \det(\mathbf{J})} \prod_{t=1}^T \frac{(-2K_{m,n})^{s_t^*}}{s_t^*! \det(\mathbf{J})^{s_t^*}} \times \quad (33)$$

$$\prod_{n=1}^N \int_0^{R_n} |h_n|^{\bar{s}_n+1} \exp \left\{ -\frac{|h_n|^2 K_{n,n}}{\det(\mathbf{J})} \right\} d|h_n|$$

$$= \sum_{s_1=0}^{s_0} \sum_{s_2=0}^{s_1} \dots \sum_{s_T=0}^{s_{T-1}} \frac{g(\mathbf{s}^*)}{\pi^N \det(\mathbf{J})} \prod_{t=1}^T \frac{(-K_{m,n})^{s_t^*}}{s_t^*! \det(\mathbf{J})^{s_t^*}} \times \quad (34)$$

$$\prod_{n=1}^N \frac{1}{2} \left(\frac{K_{n,n}}{\det(\mathbf{J})} \right)^{-\frac{\bar{s}_n}{2} - \frac{1}{2}} \left[\Gamma \left(\frac{1 + \bar{s}_n}{2} \right) - \Gamma \left(\frac{1 + \bar{s}_n}{2}, \frac{K_{n,n} R_n^2}{\det(\mathbf{J})} \right) \right],$$

where

$$g(\mathbf{s}^*) = \left(\frac{1}{2} \right)^{\sum_{t=1}^T s_t^*} \sum_{\mathbf{v} \in \mathcal{V}} \left[\prod_{t=1}^T \binom{s_t^*}{v_t} \right] (2\pi)^N \prod_{i=1}^N \mathbf{1}_{\{\Delta_i=0\}}, \quad (35)$$

and \bar{s}_n is the sum of s_t^* affecting $(|h_n| |h_m|)^{s_t^*}$. To compute \bar{s}_n , let us introduce a new matrix

$$\mathbf{S}^* = \begin{bmatrix} 0 & s_1^* & s_2^* & \dots & s_{N-1}^* \\ & & s_N^* & \dots & s_{2N-3}^* \\ \vdots & & \ddots & & \vdots \\ & & & & s_T^* \\ 0 & & \dots & & 0 \end{bmatrix}. \quad (36)$$

Using (36), we have $\bar{s}_n = \sum_{i=1}^N S_{n,i}^* + \sum_{i=1}^{n-1} S_{i,n}^* + 1$ such that $S_{i,n}^*$ is the (i, n) -th entry of \mathbf{S}^* .

APPENDIX C: OUTAGE PROBABILITY AT HIGH SNR

According to [37], the outage probability of a wireless communication system at high SNR can be obtained via the PDF of its fading channels. In particular, suppose the PDF of the channels at high SNR can be approximated as

$$f_{|h_{\text{FAS}}|}(\Omega) = 2\xi\Omega^{2M+1} + o(\Omega^{2M+1}). \quad (37)$$

Then the outage probability at high SNR is found as

$$\mathbb{P}\{|h_{\text{FAS}}| < \Omega\} = \frac{\xi}{M+1} \Omega^{2(M+1)} + o\left(\frac{1}{SNR^{M+1}}\right). \quad (38)$$

Before approximating the PDF of FAS at high SNR, we highlight that the PDF of (21) in terms of its amplitude and phase can be rewritten as

$$f_{|\mathbf{h}|, \boldsymbol{\theta}}(|h_1|, \theta_1, \dots, |h_N|, \theta_N) = \prod_{n=1}^N \frac{|h_n| H_n}{\pi^N \det(\mathbf{J})}, \quad (39)$$

where

$$H_n = \exp \left\{ -\frac{K_{n,n} |h_n|^2}{\det(\mathbf{J})} - \frac{2 \sum_{m=n+1}^N K_{m,n} |h_n| |h_m| \cos(\theta_n - \theta_m)}{\det(\mathbf{J})} \right\}. \quad (40)$$

Using (39), the approximated PDF of FAS at high SNR can be derived as

$$f_{|h_{\text{FAS}}|}(\Omega) = \frac{\partial F_{|h_{\text{FAS}}|}(\Omega)}{\partial \Omega} \quad (41)$$

$$\stackrel{(a)}{=} N \int_0^\Omega \dots \int_0^\Omega \int_0^{2\pi} \dots \int_0^{2\pi} f_{|\mathbf{h}|, \boldsymbol{\theta}}(|h_1|, \theta_1, \dots, |h_{N-1}|, \theta_{N-1}, \Omega, \theta_N) \times \quad (42)$$

$$d|h_1| \dots d|h_{N-1}| d\theta_1 \dots d\theta_N$$

$$\stackrel{(b)}{=} \frac{N\Omega}{\pi^N \det(\mathbf{J})} \int_0^{2\pi} \dots \int_0^{2\pi} H_N \int_0^\Omega |h_{N-1}| \left(H_{N-1} \times \dots \left(\int_0^\Omega |h_2| H_2 \left(\int_0^\Omega |h_1| H_1 d|h_1| \right) d|h_2| \right) d|h_{N-1}| \right) d\theta_1 \dots d\theta_N, \quad (43)$$

where (a) is obtained using Leibniz integral and (b) is obtained using (39).

According to [43], the term $\int_0^\Omega |h_n| H_n d|h_n|$ can be solved by applying Taylor series approximation at around zero. Specifically, we have

$$\int_0^\Omega |h_n| H_n d|h_n| = \frac{\Omega^2}{2} + o(\Omega^2), n = \{1, \dots, N-1\} \quad (44)$$

and the Taylor series approximation of H_N at zero is

$$H_N = 1 + o(1). \quad (45)$$

Substituting (44) and (45) into (43), we have

$$f_{|h_{\text{FAS}}|}(\Omega) = \frac{N\Omega}{\pi^N \det(\mathbf{J})} \left[\frac{\Omega^2}{2} + o(\Omega^2) \right]^{N-1} \int_0^{2\pi} \dots \int_0^{2\pi} d\theta_1 \dots d\theta_N \quad (46)$$

$$= \frac{2N}{\det(\mathbf{J})} \Omega^{2N-1} + o(\Omega^{2N-1}). \quad (47)$$

Comparing (47) to (37), we have $M = N - 1$ and $\xi = \frac{N}{\det(\mathbf{J})}$. Applying (38), we have

$$\mathbb{P}\{|h_{\text{FAS}}| < \Omega\} \approx \frac{1}{\det(\mathbf{J})} \Omega^{2N} + o\left(\frac{1}{SNR^N}\right). \quad (48)$$

APPENDIX D: DIVERSITY GAIN OF FAS

Let us consider the case where $W \rightarrow \infty$. According to [37], the diversity gain of a wireless communication system can be obtained via the PDF of its fading channels at high SNR. Specifically, suppose the PDF of the channels at high SNR can be approximated as in (37). Then diversity gain of such system is given by

$$D = M + 1. \quad (49)$$

In Appendix C, we have $M = N - 1$. Thus, it is straightforward that the diversity gain of FAS as $W \rightarrow \infty$ is N . Nevertheless, if W is finite, \mathbf{J} might be near to being singular. To see this, let us consider FAS with $N \rightarrow \infty$ ports within a finite W where each port is equally separated, and they are indexed as $1, 2, \dots$. Without loss of generality, let us focus on two ports: the n -th and $(n+1)$ -th port. The correlation between the n -th port and $(n+1)$ -th port is $\mathbf{J}_{n,n+1} = \lim_{N \rightarrow \infty} \sigma^2 J_0(2\pi \frac{1}{N-1} W) = \sigma^2 J_0(0)$, and we have $h_{n+1} = h_n$. Thus, the joint CDF of h_n and h_{n+1} is $F_{h_n, h_{n+1}}(g_1, g_2) = F_{h_n}(\min\{g_1, g_2\})$, which implies that they reduce to singularity. Since there are many such ports, we can use a finite N' ports to approximate the channels of FAS with N ports, where N' is the numerical rank of \mathbf{J}' such that \mathbf{J}' is covariance matrix as defined in (2) with $N \rightarrow \infty$ for a fixed W . As a result, the diversity gain of FAS is approximately limited by $\min\{N, N'\}$. If N is large, the same observation can be obtained. To remove the nearly-dependent entries of \mathbf{J} , one may employ rank-revealing QR factorization [44] or Gauss-Jordan elimination with a given tolerance.

REFERENCES

- [1] A. Shojaeifard, K.-K. Wong, K.-F. Tong, Z. Chu, A. Mourad, A. Haghigat, I. Hemadeh, N. T. Nguyen, V. Tapio, and M. Juntti, “MIMO evolution beyond 5G through reconfigurable intelligent surfaces and fluid antenna systems,” *Proceedings of the IEEE*, vol. 110, no. 9, pp. 1244–1265, 2022.
- [2] K. K. Wong, K.-F. Tong, Y. Shen, Y. Chen, and Y. Zhang, “Bruce Lee-inspired fluid antenna system: Six research topics and the potentials for 6G,” *Frontiers in Communications and Networks*, p. 5, 2022.
- [3] Y. Shen, K.-F. Tong, and K.-K. Wong, “Radiation pattern diversified single-fluid-channel surface-wave antenna for mobile communications,” in *2022 IEEE-APS Topical Conference on Antennas and Propagation in Wireless Communications (APWC)*, 2022, pp. 049–051.

- [4] ——, “Radiation pattern diversified double-fluid-channel surface-wave antenna for mobile communications,” in *2022 IEEE-APS Topical Conference on Antennas and Propagation in Wireless Communications (APWC)*, 2022, pp. 085–088.
- [5] ——, “Reconfigurable surface wave fluid antenna for spatial MIMO applications,” in *2021 IEEE-APS Topical Conference on Antennas and Propagation in Wireless Communications (APWC)*, 2021, pp. 150–152.
- [6] ——, “Beam-steering surface wave fluid antennas for MIMO applications,” in *2020 IEEE Asia-Pacific Microwave Conference (APMC)*, 2020, pp. 634–636.
- [7] K.-K. Wong, A. Shojaeifard, K.-F. Tong, and Y. Zhang, “Fluid antenna systems,” *IEEE Transactions on Wireless Communications*, vol. 20, no. 3, pp. 1950–1962, 2021.
- [8] K.-K. Wong, K.-F. Tong, Y. Chen, and Y. Zhang, “Extra-large MIMO enabling slow fluid antenna massive access for millimeter-wave bands,” *Electronics Letters*, vol. 58, no. 25, pp. 1016–1018, 2022.
- [9] L. Tlebaldiyeva, S. Arzykulov, K. M. Rabie, X. Li, and G. Nauryzbayev, “Outage performance of fluid antenna system (FAS)-aided terahertz communication networks,” *Accepted by 2023 IEEE International Conference on Communications (ICC)*, 2023.
- [10] M. Khammassi, A. Kammoun, and M.-S. Alouini, “A new analytical approximation of the fluid antenna system channel,” *IEEE Transactions on Wireless Communications*, pp. 1–1, 2023.
- [11] D. G. Brennan, “Linear diversity combining techniques,” *Proceedings of the IRE*, vol. 47, no. 6, pp. 1075–1102, 1959.
- [12] K. K. Wong, A. Shojaeifard, K.-F. Tong, and Y. Zhang, “Performance limits of fluid antenna systems,” *IEEE Communications Letters*, vol. 24, no. 11, pp. 2469–2472, 2020.
- [13] K.-K. Wong and K.-F. Tong, “Fluid antenna multiple access,” *IEEE Transactions on Wireless Communications*, vol. 21, no. 7, pp. 4801–4815, 2022.
- [14] C. Skouroumounis and I. Krikidis, “Large-scale fluid antenna systems with linear MMSE channel estimation,” in *ICC 2022 - IEEE International Conference on Communications*, 2022, pp. 1330–1335.
- [15] L. Tlebaldiyeva, G. Nauryzbayev, S. Arzykulov, A. Eltawil, and T. Tsiftsis, “Enhancing QoS through fluid antenna systems over correlated Nakagami-m fading channels,” in *2022 IEEE Wireless Communications and Networking Conference (WCNC)*, 2022, pp. 78–83.
- [16] K. Wong, K. Tong, Y. Chen, and Y. Zhang, “Closed-form expressions for spatial correlation parameters for performance analysis of fluid antenna systems,” *Electronics Letters*, vol. 58, no. 11, pp. 454–457, 2022.
- [17] K. N. Le, “A review of selection combining receivers over correlated rician fading,” *Digital Signal Processing*, vol. 88, pp. 1–22, 2019. [Online]. Available: <https://www.sciencedirect.com/science/article/pii/S1051200418307176>
- [18] K. S. Miller, “Complex Gaussian processes,” *Siam Review*, vol. 11, no. 4, pp. 544–567, 1969.
- [19] C. Tan and N. Beaulieu, “Infinite series representations of the bivariate Rayleigh and Nakagami-m distributions,” *IEEE Transactions on Communications*, vol. 45, no. 10, pp. 1159–1161, 1997.
- [20] P. Dharmawansa, N. Rajatheva, and C. Tellambura, “On the trivariate Rician distribution,” *IEEE Transactions on Communications*, vol. 56, no. 12, pp. 1993–1997, 2008.
- [21] Y. Chen and C. Tellambura, “Infinite series representations of the trivariate and quadrivariate Rayleigh distribution and their applications,” *IEEE Transactions on Communications*, vol. 53, no. 12, pp. 2092–2101, 2005.
- [22] M. Tekinay and C. Beard, “Moments of the quadrivariate Rayleigh distribution with applications for diversity receivers,” *Annals of Telecommunications*, vol. 75, no. 7, pp. 447–459, 2020.
- [23] Y. Chen and C. Tellambura, “Distribution functions of selection combiner output in equally correlated Rayleigh, Rician, and Nakagami-m fading channels,” *IEEE Transactions on Communications*, vol. 52, no. 11, pp. 1948–1956, 2004.
- [24] G. Karagiannidis, D. Zogas, and S. Kotsopoulos, “On the multivariate Nakagami-m distribution with exponential correlation,” *IEEE Transactions on Communications*, vol. 51, no. 8, pp. 1240–1244, 2003.

- [25] M. Wiegand and S. Nadarajah, "A series representation for multidimensional Rayleigh distributions," *International Journal of Communication Systems*, vol. 31, no. 6, p. e3510, 2018, e3510 dac.3510. [Online]. Available: <https://onlinelibrary.wiley.com/doi/abs/10.1002/dac.3510>
- [26] ——, "Series approximations for Rayleigh distributions of arbitrary dimensions and covariance matrices," *Signal Processing*, vol. 165, pp. 20–29, 2019.
- [27] ——, "New generalised approximation methods for the cumulative distribution function of arbitrary multivariate Rayleigh random variables," *Signal Processing*, vol. 176, p. 107664, 2020. [Online]. Available: <https://www.sciencedirect.com/science/article/pii/S0165168420302073>
- [28] R. G. Gallager, *Principles of digital communication*. Cambridge University Press Cambridge, UK, 2008, vol. 1.
- [29] Z. Chai, K.-K. Wong, K.-F. Tong, Y. Chen, and Y. Zhang, "Port selection for fluid antenna systems," *IEEE Communications Letters*, vol. 26, no. 5, pp. 1180–1184, 2022.
- [30] L. Zhu, W. Ma, and R. Zhang, "Modeling and performance analysis for movable antenna enabled wireless communications," *arXiv preprint arXiv:2210.05325*, 2022.
- [31] W. Ma, L. Zhu, and R. Zhang, "MIMO capacity characterization for movable antenna systems," *arXiv preprint arXiv:2210.05396*, 2022.
- [32] N. Waqar, K.-K. Wong, K.-F. Tong, A. Sharples, and Y. Zhang, "Deep learning enabled slow fluid antenna multiple access," *IEEE Communications Letters*, vol. 27, no. 3, pp. 861–865, 2023.
- [33] K.-K. Wong, K.-F. Tong, Y. Chen, and Y. Zhang, "Fast fluid antenna multiple access enabling massive connectivity," *IEEE Communications Letters*, vol. 27, no. 2, pp. 711–715, 2023.
- [34] H. Xu, K.-K. Wong, W. K. New, and K.-F. Tong, "On the outage probability for two-user fluid antenna multiple access," *Accepted by 2023 IEEE International Conference on Communications (ICC)*, 2023.
- [35] G. L. Stüber and G. L. Steuber, *Principles of mobile communication*. Springer, 1996, vol. 2.
- [36] D. Tse and P. Viswanath, *Fundamentals of wireless communication*. Cambridge university press, 2005.
- [37] Z. Wang and G. Giannakis, "A simple and general parameterization quantifying performance in fading channels," *IEEE Transactions on Communications*, vol. 51, no. 8, pp. 1389–1398, 2003.
- [38] G. Golub, A. Hoffman, and G. Stewart, "A generalization of the eckart-young-mirsky matrix approximation theorem," *Linear Algebra and its Applications*, vol. 88-89, pp. 317–327, 1987. [Online]. Available: <https://www.sciencedirect.com/science/article/pii/0024379587901145>
- [39] D. Dowson and B. Landau, "The Frechet distance between multivariate normal distributions," *Journal of Multivariate Analysis*, vol. 12, no. 3, pp. 450–455, 1982. [Online]. Available: <https://www.sciencedirect.com/science/article/pii/0047259X8290077X>
- [40] S. Boyd, S. P. Boyd, and L. Vandenberghe, *Convex optimization*. Cambridge university press, 2004.
- [41] W. Ford, *Numerical linear algebra with applications: Using MATLAB*. Academic Press, 2014.
- [42] A. Papoulis and S. U. Pillai, "Probability, random variables, and stochastic processes," 2002.
- [43] S. Liu, J. Cheng, and N. C. Beaulieu, "Asymptotic error analysis of diversity schemes on arbitrarily correlated Rayleigh channels," *IEEE Transactions on Communications*, vol. 58, no. 5, pp. 1351–1355, 2010.
- [44] G. Golub, "Numerical methods for solving linear least squares problems," *Numerische Mathematik*, vol. 7, no. 3, pp. 206–216, 1965.